Numerical Study of Ground Surface Settlement Induced by Diaphragm and Buttress Installation

A. Lim[1] and P. Hsieh[2]

[1]*Department of Civil Engineering, Universitas Katolik Parahyangan, Bandung, Indonesia*

[2]*Department of Assets and Property Management, Hwa Hsia University of Technology, New Taipei City, Taiwan*

E-mail: spg@cc.hwh.edu.tw

ABSTRACT: In construction practices, diaphragm walls are a cast-in-situ reinforced concrete retaining wall that is constructed using a slurry supported trench method. The installation process includes slurry supported trench excavation, placing the reinforcement cage, concrete casting and curing. This installation process would modify the in-situ stress state in the soil close to the trench and generate ground surface settlements, which might be significant compared to those induced by the main excavation. Also, the construction of buttress walls, a concrete wall that perpendicular to diaphragm walls, might generate additional ground surface settlement, and this issue has not been investigated. For clarify this issue, a series of three-dimensional finite element analysis was performed to quantify the amount of ground surface settlement induced by the diaphragm and buttress walls installation process using the Wall Installation Modeling (WIM) method. Results show that the installation of buttress walls inside or outside the excavation zone did not yield significant additional ground surface settlement outside the excavation zone because the diaphragm wall was completed first before the construction of the buttress wall. But, the construction of outer buttress walls could widen the settlement zone.

KEYWORDS: Excavation, Settlement, Installation, Buttress wall, Diaphragm wall.

1. INTRODUCTION

In construction practices, diaphragm/buttress/cross walls are a cast-in-situ reinforced concrete retaining wall constructed using a slurry supported trench method. The installation process includes slurry supported trench excavation, placing the reinforcement cage, concrete casting and curing. This installation process would modify the in-situ stress state in the soil close to the trench and generate ground surface settlements, which might be significant compared to those induced by the main excavation.

The installation effects of diaphragm wall have been investigated using the three-dimensional numerical analyses and found that the soil stress redistribution might be generated due to the installation of diaphragm walls and its quality of construction (Gourvenec and Powrie 1999, Ng and Yan 1999, Comodromos et al. 2013). Schäfer and Triantafyllidis (2006) compared the results from the Wall-Installation-Modelled (WIM) method and the Wished-In-Place (WIP) method using three-dimensional finite element analysis of TNEC excavation project in Taipei basin (Ou et al. 1998). They concluded the WIP method would underestimate 15-20% of the ground surface settlements and the wall deflections compared to the WIM method. Also, the construction of buttress walls might generate an additional ground surface settlement, and this issue has not been investigated.

For clarify this issue, three-dimensional finite element analyses (Brinkgreve et al., 2013) were performed to quantify the amount of ground surface settlement induced by the diaphragm and buttress walls installation process using the WIM method.

2. CURRENT PRACTICE OF USING BUTTRESS WALLS

Nowadays, the application of buttress walls has been expanded, not only as an auxiliary measure to control excessive deformations induced by excavation (Ou et al. 2006, Lin and Woo 2007, Ou et al. 2008, Hwang et al 2008, Chen et al. 2011, Hsieh et al. 2015, Hsieh et al. 2016, Lim et al 2016, Lim et al 2018) but also as a part of a strut-free retaining system (Hsieh et al. 2011, Chuah and Tan, 2010, Lim and Ou 2018). Figure 1 illustrates the layout of cross walls and buttress walls. The buttress wall is a concrete wall perpendicular to the diaphragm wall constructed before excavation, and it is not connected to the opposite diaphragm wall. Moreover, the construction technique and equipment of cross walls and buttress walls are similar to the construction technique and apparatus of diaphragm walls (Ou et al. 2006).

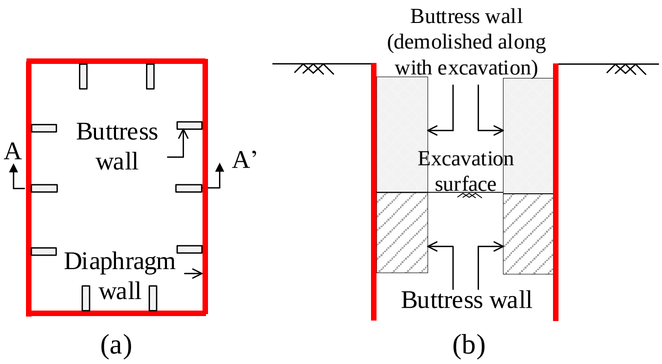

Figure 1 Schematic diagram of buttress walls and cross walls a) Plan view, b) Cross-section view

2.1 Buttress walls as an auxiliary measure

Ou et al. (2006) presented an ideal case history of deep excavation (the UPIB building) which utilizing cross wall and buttress wall as a protection measure to the adjacent building during excavation based on field observations and numerical analysis results. This case history has a good monitoring record, great construction quality, and well-documented construction sequence. Based on monitoring results, the cross wall can reduce the diaphragm wall movement and ground settlement significantly. Such behavior was similar to the three-dimensional response of the diaphragm wall near the corner in an excavation. The design of cross wall spacing can resort to three-dimensional numerical analysis or empirical formula with the consideration of the diaphragm wall corner effect.

Hwang and Moh (2008) evaluated the effectiveness of buttresses and cross walls in reducing deflections of diaphragm walls in two cases by studying the wall deflection paths and reference envelopes. Both sites are located in the K1 Zone of the Taipei Basin, and excavations were carried out to a depth of 32 m by using the top-down method of construction. It found that cross walls were effective in reducing wall movements in these two cases. On the other hand, the effectiveness of buttresses was highly dependent on their configurations. The buttress wall with an average width of 3.5 m was out of performing. Meanwhile, the buttress wall with length 6 to 15 m showed a promising result in reducing diaphragm wall movement.

Ou et al. (2008) performed parametric studies by using three-dimensional finite element analysis of an excavation case history with buttress walls. It revealed that the deflection of the diaphragm wall was strongly influenced by the condition of the restraint at the bottom of the buttress walls, and by the number of buttress walls. As long as the buttress wall bottom was well restrained, and reasonable quantities of buttress walls were installed, wall deflection can be considerably reduced.

Chen et al. (2011) examined the influence of the geometry of the buttress walls (shape, thickness, and length) on the displacement of buttressed diaphragm wall via a series of three-dimensional analysis. The results indicated that the adequate spacing of the buttress walls should be within two times the excavation depth and that the T-shaped buttress wall was more efficient than the I-shaped buttress walls.

Hsieh et al. (2015) performed a case study regarding the design of excavation with the installation of buttress walls. They combined both observation and prediction to establish a numerical model and investigated the efficiency of buttress walls. They concluded that required buttress wall length is not fixed and should be designed according to the difference between the predicted diaphragm wall deflections and the controlled value. Also, the condition of groundwater level within the excavation zone due to diaphragm wall construction and the simulation of the adjacent buildings should be appropriately taken into account in the analysis.

Hsieh et al. (2016) performed three-dimensional finite element analyses of two excavation case histories. Then, a series of the parametric study was conducted by varying soil types, types and length of buttress walls based on the evaluated case histories. Results show that the mechanism of buttress walls in reducing wall deflections mainly came from the frictional resistance between the side surface of buttress wall and adjacent soil rather than from the combined bending stiffness from the diaphragm and buttress walls. The rectangular shape of buttress walls was a better effect than T-shape in the shallow excavation because the frictional resistance between buttress walls and adjacent soil played a significant role in reducing the wall deflection rather than bearing resistance of the flange. When the excavation went more in-depth, the difference in reducing the wall deflection between the R-shape and T-shape became small.

2.2 Buttress walls as a part of a strut-free retaining system

Chuah and Tan (2010) highlighted the new earth retention strut-free scheme for excavation using counterfort diaphragm wall in a Singapore excavation project. The excavation depth of this project was around 8 m, and the subsurface condition was mainly thick soft soils deposit. These counterfort walls in thick soft soils deposit were founded on good base support for it to work well without any strut or tied-back system. The width of counterfort wall was 4 m and 7 to 7.5 m spacing. They were located inside excavation zone, surrounding the diaphragm wall, and were connected by 0.3 m thick of counterfort slabs. Although this excavation was successfully constructed, the deformations were not easy to be controlled. They suggested other mitigation measures such as additional layers of struts or tied-back at the top of the wall may be required to avoid excessive wall deflection at the top. In other words, this technique was not intended to be adopted where the deformations was a critical issue.

Hsieh et al. (2011) demonstrated the successful use of T-shaped diaphragm wall as the retaining system of a large-scale deep excavation project. Lateral displacement of the T-shaped diaphragm wall was kept within 1.5 cm when the intended excavation depth of 9.6 m was reached. The adjacent buildings suffered only minor non-structural damages due to settlement induced by a combined effect of excavation and dewatering. It was explained that the T-shaped diaphragm wall depends on its flexural stiffness and side friction to withstand the unbalanced forces. However, the usage of the T-shaped diaphragm wall only limit the good soil conditions (medium to dense sand) and the depth of excavation is relatively shallow such as 9 meters at most.

Lim and Ou (2018) presented a case history in New Taipei city, which adopted several types of buttress walls combined with diaphragm wall as a strut-free retaining wall system. The soil layers above the final excavation level are dominated by the soft to medium clay layer (NSPT=2-7) and the loose silty sand layer (NSPT=2-6). This project was successfully constructed with the ratio of the maximum wall deflection to excavation depth equal to 0.55% and the maximum ground surface settlement was 27 mm. The success of this project was also contributed from the low groundwater level (i.e., GL -10 m). According to numerical analysis, when the groundwater level raised from GL -10 m to GL -2 m, the maximum wall deflection increased by 180% from the original result and make this system might not be feasible to be adopted.

3. SOIL CONSTITUTIVE MODEL

The Hardening Soil model (Schanz et al. 1999), abbreviated as the HS model, is a true second-order model for soil in general (soft to stiff types of soil). The model involves frictional hardening characteristics to model the plastic shear strain in deviatoric loading, and cap hardening characteristics to model the plastic volumetric strain in the primary compression. The Mohr-Coulomb failure criterion defines failure. The essential features of the model are a Mohr-Coulomb failure with input parameters c, ϕ and dilatancy angle, ψ, stress-dependent stiffness according to a power-law defined by input parameter, m, plastic straining resulting from primary deviatoric loading with an input parameter, E_{50}^{ref}, and plastic straining from primary compression with an input parameter E_{oed}^{ref}, elastic unloading/reloading is defined by input parameters E_{ur}^{ref} and unloading/reloading Poisson's ratio, υ_{ur}.

Figure 2 displays the shear yield surface and cap yield surface in the Hardening Soil Model for soil with no cohesion ($c'=0$). The soil yield is defined as the stress state of soil which is located in the shear hardening zone. Meanwhile, the soil failure is defined as the stress state of soil which reaches to the Mohr-Coulomb failure line.

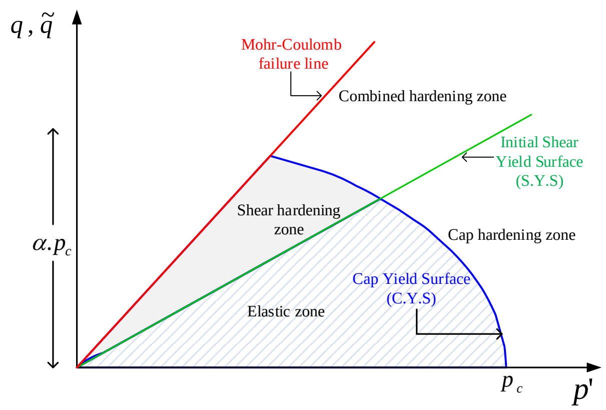

Figure 2 Shear yield surface and cap yield surface in the Hardening Soil Model (Lim and Ou, 2017)

Furthermore, Figures 3(a) and 3(b) illustrate the hyperbolic stress-strain relation in primary loading for a standard drained triaxial test and oedometer test, respectively, to express the definition of E_{50}^{ref}, E_{ur}^{ref}, and E_{oed}^{ref}.

The HS model is difficult to accurately predict the drop in the deviator stress, which represents a strain-softening response of soil behavior. Nevertheless, regarding an effective stress path, the typical shape of the normally consolidated clay stress paths, and their undrained shear strength are handled very well by the HS model predictions (Surarak et al., 2012). In other words, the HS model can represent real soil behavior as long as the soil response is a strain hardening behavior.

In the analyses of fine-grained soils (undrained conditions), an elastic unloading/reloading Young's modulus was mathematically derived based on a result of oedometer tests (Lim and Ou 2017), as shown in Eq. (1), which e is void ratio, p' is mean effective stress, $\kappa = C_s/\ln 10$, and C_s is swelling index.

$$E_{ur} = \frac{3(1+e)p'(1-2\upsilon_{ur})}{\kappa} \tag{1}$$

To be used as an input parameter in the HS model E_{ur} should be converted to the E_{ur}^{ref} as proposed by Schanz et al. (1999), as shown in Eq. (2).

$$E_{ur} = E_{ur}^{ref}\left(\frac{c.\cos\phi - \sigma'_3 \sin\phi}{c.\cos\phi + p_{ref}\sin\phi}\right)^m \tag{2}$$

When E_{ur}^{ref} is determined, then $E_{50}^{ref} = 1/3E_{ur}^{ref}$ and $E_{oed}^{ref} = 0.7E_{50}^{ref}$ can be estimated as suggested by Calvello and Finno (2004).

In the analyses of coarse-grained soils (drained conditions), the modulus parameters were obtained according to Khoiri and Ou (2013), as shown in Eq. (3), which E_s is Young's modulus of fine-grained soils (unit: kPa).

$$E_s = (2000-4000)N_{SPT} \tag{3}$$

To be used as an input parameter in the HS model, E_s should be converted to the E_{ur}^{ref}, as shown in Eq. (4).

$$E_{ur}^{ref} = E_s / (\sigma_3' / p_{ref})^m \tag{4}$$

When E_{ur}^{ref} is determined, then $E_{50}^{ref} = 1/3E_{ur}^{ref}$ and $E_{oed}^{ref} = 1.5E_{50}^{ref}$ can be estimated as suggested by Khoiri and Ou (2013).

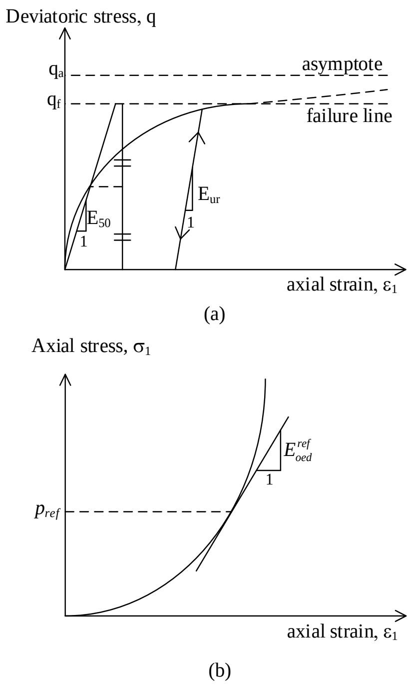

Figure 3 The stress-strain relation in primary loading for a) a standard drained triaxial test, b) oedometer test (Brinkgreve et al., 2013)

4. WALL INSTALLATION MODELLING (WIM) METHOD

The WIM method analysis followed the procedures which were done by Schäfer and Triantafyllidis (2006). Figure 4 presents the three-dimensional finite element model for the WIM model.

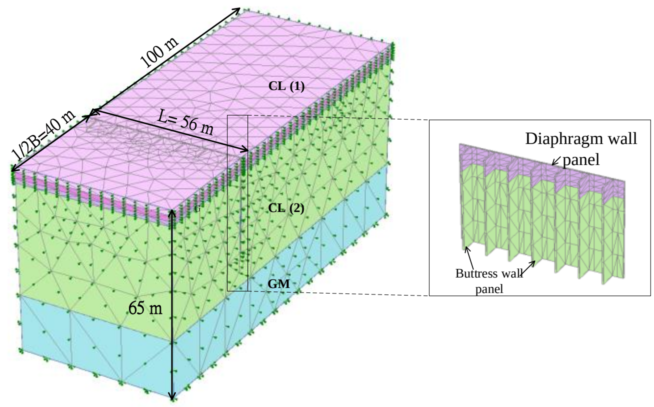

Figure 4 Finite element model for the WIM model analysis

The depth of the trench (H_t) was 33 m, and the excavation length was 56 m. The model represents a plane section which comprises fifteen diaphragm wall panels and seven buttress wall panels. The Hardening Soil (HS) model (Schanz et al, 1999) was adopted to simulate the soil behavior, including the clay (CL) and the silty gravel (GM) under the undrained and drained conditions, respectively. The model parameters of soils were typical values for the Taipei silty clay and the Taipei silty gravel (Lim and Ou 2017; Hsieh et al 2016). Table 1 lists the input parameters for the WIM model analysis. 10-node tetrahedral elements were employed to simulate the soil and trench volume. Soil movements normal to the four vertical sides were restrained while they were restrained in all directions at the bottom of the geometry.

Table 1 Soil input parameters for analyses

Soil layer	Depth (m)	γ_t (kN/m^3)	ϕ' (deg)	E_{50}^{ref} (kPa)	E_{oed}^{ref} (kPa)	E_{ur}^{ref} (kPa)	m
CL(1)	0 - 2	18.25	30	7033	4923	21100	1
	2 - 4	18.25	30	6826	4779	20479	1
	4 - 5.6	18.25	30	6631	4642	19894	1
CL(2)	5.6 - 45	18.5	30	9488	6642	28470	1
GM	45 - 65	19.6	37	85000	121000	256000	0.5

Note: $R_f = 0.9$; $\upsilon_{ur} = 0.2$

The plane section of the considered diaphragm wall consists of fifteen diaphragm wall panels and seven buttress wall panels with a selected length of 4 m and 6 m, respectively, as shown in **Figure 5**. The thickness of the diaphragm and buttress walls was assumed 0.6 m. A number nearby each panel indicates the construction stage, for example, the panel H was first constructed (stage 1), followed by the panel D and the panel L (stage 2), then the panel A and the panel O (stage 3), and so forth. After all of the diaphragm wall panels were completed, then the panel buttress-H was constructed (stage 8), followed with the panel buttress-D and the panel buttress-L (stage 9), and closed by the panel buttress-B, the panel buttress-F, the panel buttress-J and the panel buttress-N (stage 10).

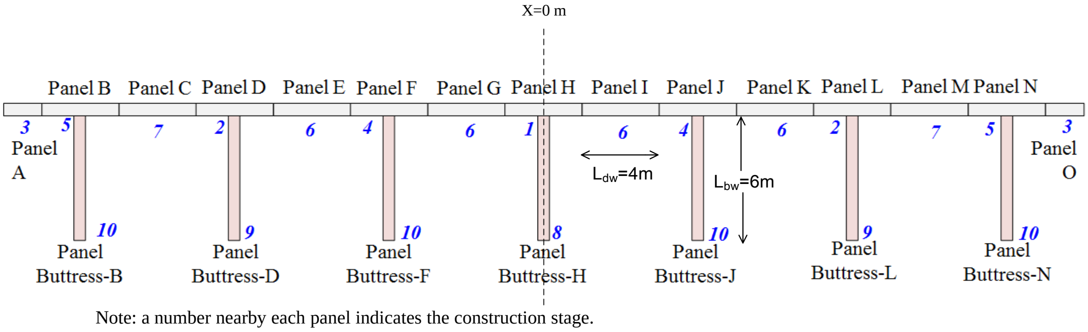

Figure 5 Construction stages of the diaphragm wall and buttress wall panels

For each stage, three additional steps should be conducted to model the WIM method such as:

1. The excavation under slurry support was modeled by deactivating the respective finite elements inside the trench and applying the distributed loads on the surface of the trench walls. The magnitude of the loads corresponds to the hydrostatic slurry pressure with a bulk unit weight of γ_b=10.3 kN/m^3.

2. On the subsequent process of concrete pouring, the distributed loads were increased from the slurry to the fresh concrete pressure (σ_c). The pouring process was modeled following the bilinear approximation by Lings et al. (1994), which adopts a hydrostatic pressure distribution up to a critical depth (h_{crit}) of 20–30% of the panel depth. Below h_{crit}, the pressure gradient corresponds to bulk unit weight γ_b of the bentonite slurry:

$$\sigma_c = \begin{cases} \gamma_c \times z, z \le h_{crit} \\ \gamma_b \times z + (\gamma_c - \gamma_b) \times h_{crit}, z > h_{crit} \end{cases} \tag{4}$$

where γ_c is the bulk unit weight of the concrete, γ_b the bulk unit weight of the slurry, z the depth below surface ground level.

3. The finite elements representing the fresh concrete were activated inside the trench, and the distributed loads are removed. The increased stiffness of the concrete due to aging is considered by a suitable evolution of Young's modulus, E, and the Poisson ratio, υ, in the course of 28 days.

5. RESULTS AND DISCUSSIONS

As shown in Figure 6, the installation of buttress walls inside the excavation zone did not yield significant ground surface settlement outside the excavation zone. However, it could generate the ground surface settlement inside the excavation zone.

Furthermore, buttress walls also modeled outside the excavation zone. As shown in Figure 7, based on the maximum settlement point of view, the installation of outer buttress walls yielded insignificant additional ground surface settlements outside the excavation zone. But, the construction of outer buttress walls widened the settlement zone.

Table 2 summarizes the maximum ground surface settlement induced by the diaphragm and buttress walls installation inside and outside the excavation zone. The maximum ground surface settlement occurred at the center of the diaphragm wall section (x=0). The maximum ground surface settlement induced by diaphragm wall installation was 16 mm. It was apparent that the installation of seven inner and outer buttress walls only increased to 1.1 mm and 0.6 mm of ground surface settlements, respectively, and they were minimal. The inner buttress wall trench excavation only induced ground surface settlement in the excavated zone but it was not necessary to be considered because the soil would be excavated soon after the retaining wall system was constructed. Moreover, the outer buttress wall trench excavation widened the ground settlement zone but the additional ground surface settlement induced by the outer buttress walls trench excavation was insignificant. Thus, it could be concluded that the installation of buttress walls has no significant effect on the additional ground surface settlement induced by the buttress walls trench excavation because the diaphragm wall was completed first before the construction of the buttress wall.

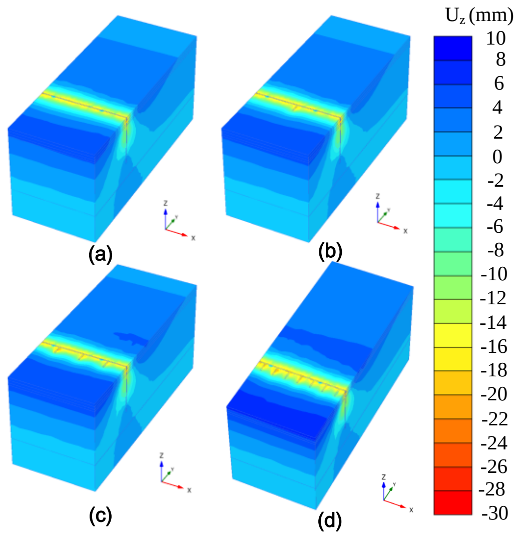

Figure 6 The contour of ground surface settlements induced by a) diaphragm wall installation, b) diaphragm wall with single inner buttress wall installation, c) diaphragm wall with three inner buttress walls installation, d) diaphragm wall with seven inner buttress walls installation

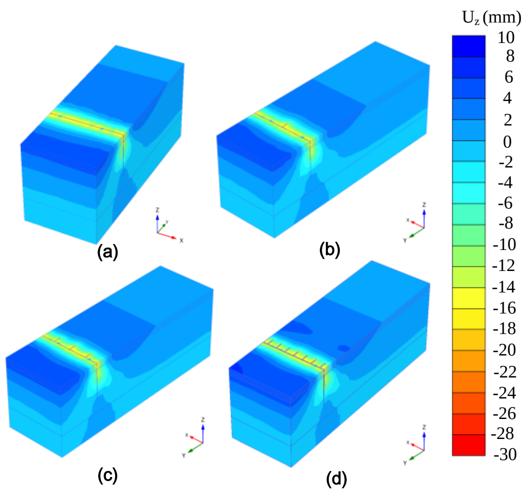

Figure 7 The contour of ground surface settlements induced by a) diaphragm wall installation, b) diaphragm wall with single outer buttress wall installation, c) diaphragm wall with three outer buttress walls installation, d) diaphragm wall with seven outer buttress walls installation

Table 2 Summary of the maximum ground surface settlement induced by the diaphragm and buttress walls installation

Description	Settlement behind the D-wall (mm)						
	x = 0 m	x = 4 m	x = 8 m	x = 12 m	x = 16 m	x = 20 m	x = 24 m
D-wall only	16.0	11.3	14.8	11.8	12.4	11.8	15.5
D-wall + 1 Inner B-wall	16.5	11.4	15.0	11.9	12.5	11.9	15.5
D-wall + 3 Inner B-walls	16.6	11.3	15.3	12.2	12.9	12.3	15.8
D-wall + 7 Inner B-walls	17.1	11.8	15.9	12.8	13.4	12.7	16.3
D-wall + 1 Outer B-wall	16.2	13.5	15.2	11.4	13.7	11.3	15.3
D-wall + 3 Outer B-walls	16.3	13.3	15.5	11.8	14.3	11.9	15.6
D-wall + 7 Outer B-walls	16.6	13.6	16.0	12.10	14.7	12.1	16.5

Note: x indicates the distance away from the center section of the diaphragm wall

Furthermore, the ground surface settlements at each cross-section of the diaphragm wall with inner and outer buttress walls were plotted in Figure 8 and Figure 9, respectively. The ground surface settlement (δ_{vw}) and the distance behind the diaphragm wall (d) are normalized with the depth of the trench (H_t). The main influence range of settlement was 0.3 to 0.5H_t from the diaphragm wall trench panel, and small settlement occurred beyond 1.0H_t from the panel. This observed settlement characteristic was also reported by Ou and Yang (2000) in which they monitored the settlement induced by the construction of the diaphragm walls for the excavations in the Taipei Rapid Transit System. In addition, at some cross-sections, small amount of ground surface heave was detected from the computation results, especially at the location between 0.5 to 1.0 d/H_t.

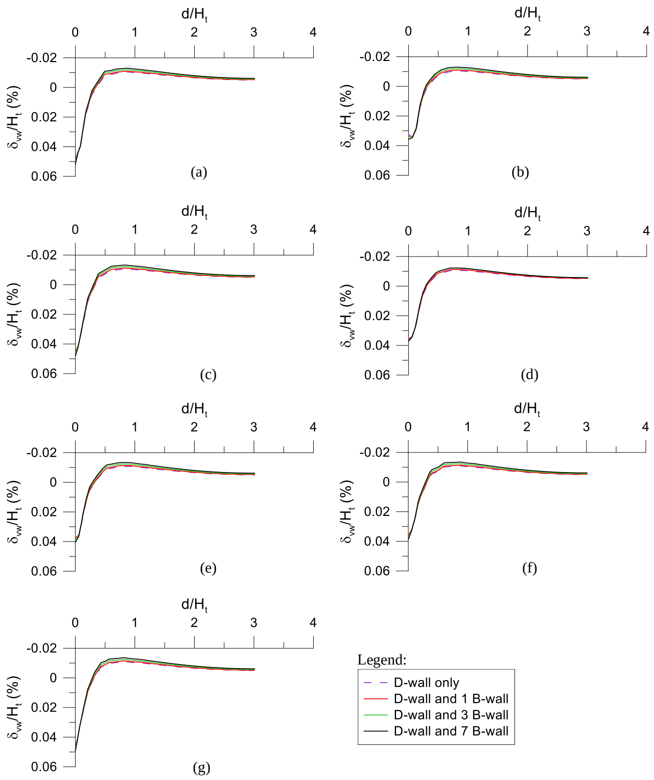

Figure 8 Profile of ground surface settlements at each cross section of the diaphragm wall and inner buttress walls a) x = 0 m, b) x = 4 m, c) x = 8 m, d) x = 12 m, e) x = 16 m, f) x = 20 m, g) x = 24 m

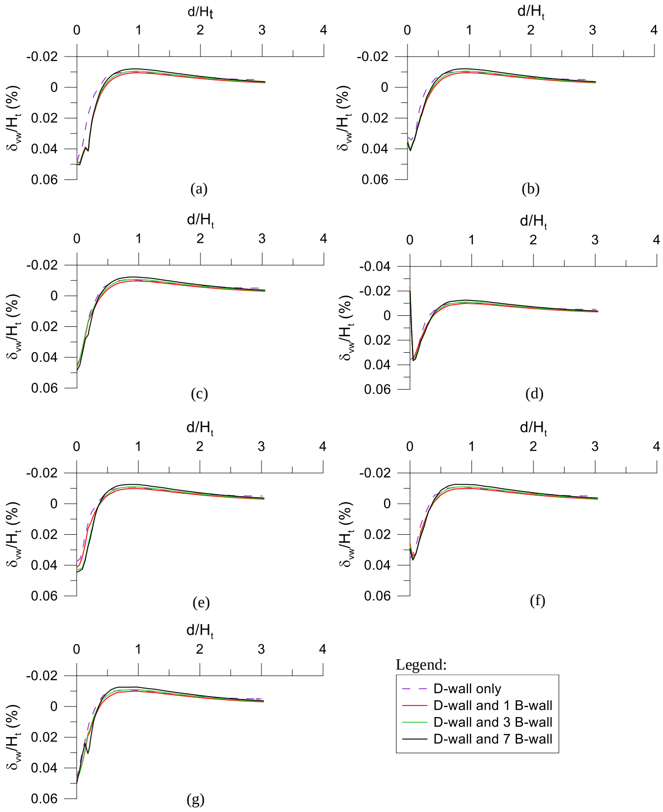

Figure 9 Profile of ground surface settlements at each cross section of the diaphragm wall and outer buttress walls a) x = 0 m, b) x = 4 m, c) x = 8 m, d) x = 12 m, e) x = 16 m, f) x = 20 m, g) x = 24 m

According to author experiences, it seems that the ground heave was unlikely to occur in the field. The possible reason might due to the limitation of HS model. Moreover, the WIM method yielded the δ_{vw} was 0.05% Ht while Ou and Yang (2000) reported the δ_{vw} was in the range of 0.05% to 0.13% H_t, depends on the progress of completed diaphragm panels. Although the computed δ_{vm} might underestimate the field condition, at least the installation effect of buttress walls could be well captured.

6. CONCLUSIONS

This study performed a series of 3D finite element analyses to quantify the amount of ground surface settlement induced by the diaphragm and buttress walls installation process using the Wall-Installation-Modelling (WIM) method. The following conclusions can be drawn:

1. The maximum ground surface settlement induced by diaphragm wall installation was 16 mm. In addition, it was apparent that the installation of seven inner and outer buttress walls only increased to 1.1 mm and 0.6 mm of ground surface settlements, respectively. This number was insignificant.
2. The inner buttress wall trench excavation only induced ground surface settlement in the excavated zone but it was not necessary to be considered because the soil would be excavated soon after the retaining wall system was constructed.
3. The outer buttress wall trench excavation widened the ground settlement zone but the additional ground surface settlement induced by the outer buttress walls trench excavation was insignificant.
4. The installation of buttress walls has no significant effect on the additional ground surface settlement induced by the buttress walls trench excavation because the diaphragm wall was completed first before the construction of the buttress wall.

5. The Wall-Installation-Modelling method would substantially increase the complexity and the running time of the analysis. Hence, for simplification, the widely used Wish-In-Place method (Hsieh et al. 2016, Dong et al. 2016, Goh et al. 2017) was adequate for the simulation of diaphragm wall and buttress wall with the consideration of the weight of the concrete from the diaphragm wall and buttress wall over the existing soil.

7. ACKNOWLEDGMENTS

The authors acknowledge the support provided by the Ministry of Science and Technology in Taiwan via grant number: MOST 106-2221-E-146-002.

8. REFERENCES

Brinkgreve, R. B. J., Engin, E., and Swolfs, W. M. (2013) "PLAXIS 3D Manual; Delft, Netherlands" PLAXIS.

Calvello, M., and Finno, R. (2004) "Selecting parameters to optimize in model calibration by inverse analysis", Computer and Geotechnics 31(5), pp410-424.

Chen, S. L., Ho, C. T., Li, C. D., Gui, M. W. (2011) "Efficiency of buttress walls in deep excavations", Journal of Geoengineering 6(3), pp145-156

Chuah, S. S., and Tan, S. A. (2010) "Numerical study on a new strut-free counterfort embedded wall in Singapore", Earth Retention Conference. ASCE, pp740-747.

Comodromos, E. M., Papadopoulou, M. C., and Konstantinidis, G. K., (2013) "Effects from diaphragm wall installation to surrounding soil and adjacent buildings", Computer and Geotechnics, 53, pp106–121.

Dong, Y. P., Burd, H. J., and Houlsby, G. T. (2016) "Finite-element analysis of a deep excavation case history", Geotechnique, 66(1), pp1–15.

Goh, A. T. C., Zhang, F., Zhang, W., and Chew, O. Y. S. (2017) "Assessment of strut forces for braced excavation in clays from numerical analysis and field measurements", Computer and Geotechnics, 86, pp141-149.

Gourvenec, S. M., and Powrie, W. (1999) "Three-dimensional finite-element analysis of diaphragm wall installation", Geotechnique, 49(6), pp801-823.

Hsieh, H. S, Wu, L. H, Lin, T. M, Cherng, J. C, and Hsu, W. T. (2011) "Performance of T-shaped diaphragm wall in a large scale excavation", Journal of GeoEngineering 6(3), pp135-144.

Hsieh, P. G, Ou, C. Y., Lin, Y. K., and Lu, F. C. (2015) "Lesson learned in design of an excavation with the installation of buttress walls", Journal of GeoEngineering 10(2), pp63-73.

Hsieh, P. G, Ou, C. Y, and Hsieh, W. H. (2016) "Efficiency of excavations with buttress walls in reducing the deflection of the diaphragm wall", Acta Geotechnica. 11, pp1087-1102. doi:10.1007/s11440-015-0416-6

Hwang, R. N., and Moh, Z. C. (2008) "Evaluating effectiveness of buttresses and cross walls by reference envelopes", Journal of GeoEngineering 3(1), pp1-11.

Khoiri, M., and Ou, C. Y. (2013) "Evaluation of deformation parameter for deep excavation in sand through case histories", Computers and Geotechnics 47(1), pp57-67.

Lim, A., Hsieh, P. G., and Ou, C. Y. (2016) "Evaluation of buttress wall shapes to limit movements induced by deep excavation", Computer and Geotechnics 78, pp155-170

Lim, A., and Ou, C. Y. (2017) "Stress paths in deep excavations under undrained conditions and its influence on deformation analysis", Journal of Tunneling and Underground Space Technology. 63, pp118-132.

Lim, A., and Ou, C. Y. (2018) "Performance and three-dimensional analyses of a wide excavation in soft soil with strut-free retaining system: case study", International Journal of Geomechanics. https://doi.org/10.1061/(ASCE)GM.1943-5622.0001165

Lim, A., Ou, C. Y., and Hsieh, P. G. (2018) "Investigation of the integrated retaining system to limit deformations induced by deep excavation", Acta Geotechnica 13, p973.

Lin, D. G, and Woo, S. M (2007) "Three Dimensional Analyses of Deep Excavation in Taipei 101 Construction Project", Journal of GeoEngineering 2(1), pp29-41

Lings, M. L., Ng, C. W. W., and Nash, D. F. T. (1994) "The lateral pressure of wet concrete in diaphragm wall panels cast under bentonite", Proceedings of the Institution of Civil Engineers Geotechnical Engineering, 107(3), pp163–172.

Ng, C. W. W., and Yan, R. W. M. (1999) "Three-dimensional modelling of a diaphragm wall construction sequence", Geotechnique, 49(6), pp825-834.

Ou, C. Y., Liao, J. T., and Lin, H. D. (1998) "Performance of Diaphragm Wall Constructed Using Top-Down Method", Journal of Geotechnical Engineering and Geoenvironmental Engineering 124, pp798-808.

Ou, C. Y., and Yang, L. L. (2000) "Ground movement induced by the construction of diaphgram wall", Geotechnical Research Report No GT200005, Department of Construction Engineering, National Taiwan University of Science and Technology, Taipei, Taiwan, R.O.C

Ou, C. Y, Lin, Y. L., and Hsieh, P. G. (2006) "Case record of an excavation with cross walls and buttress walls", Journal of GeoEngineering 1(2), pp79-86.

Ou, C. Y., Teng, F. C, Seed, R. B, and Wang, I. W. (2008) "Using buttress walls to reduce excavation-induced movements", Proceedings of the Institution of Civil Engineers Geotechnical Engineering 161(GE4), pp209–222

Schäfer, R., and Triantafyllidis, T. (2006) "The influence of the construction process on the deformation behaviour of diaphragm walls in soft clayey ground", International Journal for Numerical and Analytical Methods in Geomechanics. 30, pp563-576.

Schanz, T., Vermeer, P. A., and Bonnier, P. G. (1999) "Formulation and verification of the Hardening-Soil model", Beyond 2000 in Computational Geotechnics. Brinkgreve ed, Rotterdam Balkema, pp281-290.

Surarak, C., Likitlersuang, S., Wanatowski, D., Balasubramaniam, A., Oh, E., and Guan, H. (2012) "Stiffness and strength parameters for hardening soil model of soft and stiff Bangkok Clays", Soils and Foundations 52(4), pp682–697.